Proceedings of ICRC 2001: 2923 © Copernicus Gesellschaft 2001

ICRC 2001

# Wavelet analysis of EGRET data

**R. Terrier**[1], **L. Demanet**[2], **I. A. Grenier**[1], **and J. P. Antoine**[2]

[1]Université Paris VII & Sap CEA Saclay
[2]Institut de physique théorique et mathématique, Université catholique de Louvain, Louvain-la-Neuve

**Abstract.** A powerful analysis method, based on wavelet transforms (WT), was developed and applied to the search of point and extended sources in the EGRET data. The exposure and PSF of EGRET vary strongly over the field of view and the galactic gamma-ray background presents many point-like structures, making the source extraction in the wavelet space difficult. A mathematical approach have been studied to successfully estimate the significance level of the wavelet coefficients. The performance of the method will be presented as well as strategy for the future GLAST mission involving an order of magnitude more sources.

## 1 Introduction

The standard EGRET analysis uses the maximum likelihood method to find point sources and estimate their fluxes and positions (see Mattox et al. (1996), Hartman et al. (1999)). It is very well suited for these problems. The next high energy $\gamma$-ray telescope, GLAST, will have a sensitivity more than 20 times larger than EGRET, and will therefore be able to detect EGRET faintest sources in one day. Several thousand sources should be discovered during the lifetime of GLAST. An efficient algorithm that can locate transient sources quickly and sensitively after data downlink is needed. Our purpose here is to develop a wavelet method well suited to search for high energy $\gamma$-rays point sources and test it on EGRET data.

Wavelets have already been used to analyze EGRET data (Dixon et al. , 1998), essentially to search for extended emission. The algorithm used, TIPSH (Kolaczyk & Dixon , 2000), is a rigorous approach to the Poisson nature of the data. It allows exact statistical calculations even in the case of a complex non-flat background. But it is limited to the two dimensional Haar wavelet which does not take into account the spatial information of the data, such as the point-spread-function (PSF) shape. Some methods have also been developped for x-ray image analysis to look for point and extended sources (Starck & Pierre (1998), Damiani et al. (1997)). These methods use isotropic wavelets which are well suited for the detection of PSF-shaped distributions. Typically, to extract the statistical significance of a wavelet transform these authors compute the local background with the density of photons at the considered point and suppose a locally flat background. But for high energy $\gamma$-ray maps, some special care is needed because of the strongly varying exposure and the bright and structured diffuse galactic emission (Hunter et al. , 1997) which make a locally flat background hypothesis wrong. Our approach here is to use the spatial information of the PSF and to deal efficiently with the complex diffuse background. We will first describe which analyzing wavelet best suits our problem, then detail the statistics of the wavelet transform of a complex diffuse background. Finally, we give a few preliminary examples of source detection in EGRET data.

*Correspondence to:* R. Terrier (terrier@cdf.in2p3.fr)

## 2 Continuous wavelet transform

Wavelet analysis has numerous interesting features for point source searches, among which are:

- Wavelets have zero mean, thus any uniform noise will be filtered to zero in average.
- The wavelet transform offers a multiscale decomposition of data. Flattened structures are not on the same footing as point-like sources and are indeed detected at different scales.

Since the EGRET PSF is strongly dependent on energy, ($\theta_{67} = 5.85^\circ (E/100\mathrm{MeV})^{-0.534}$ Thompson et al. (1993)), so are the typical scales of point sources. Therefore, we consider that continuous wavelet transform ( hereafter CWT ) is more suited than the discrete wavelet transform for our particular problem. The former allows us to consider the data at *every* scale, whereas the later is restricted to dyadic scales. With $L^\infty$ normalization, the wavelet transform of a given image s, for a given point $b$ and a given scale $a$ is (Antoine et

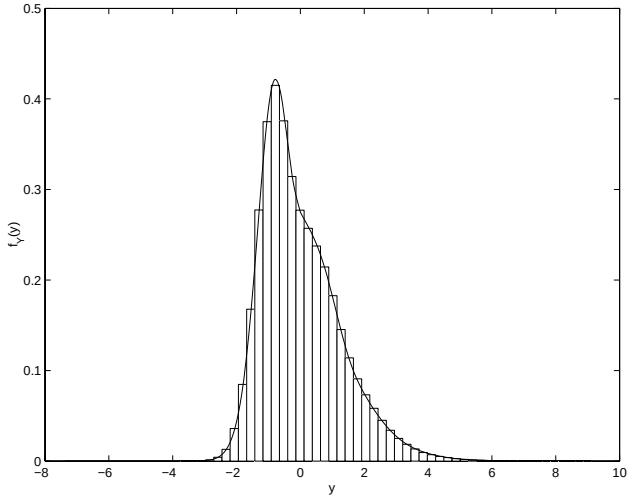


**Fig. 1.** Probability density function of the wavelet transform values for a low intensity background computed directly from expression (3) (solid line). The histogram gives the values obtained by simulation.

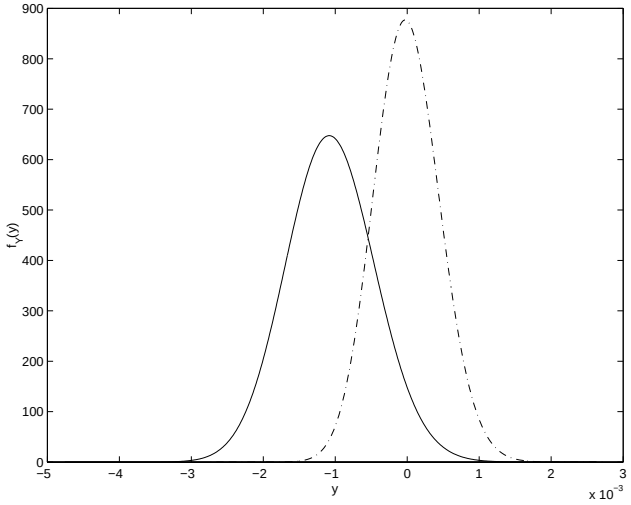


**Fig. 2.** Probability density function of the wavelet transform values near a strong background bump. Dash dotted line is obtained supposing a flat background, solid line using the direct computation. It will give smaller thresholds because of the negative ring around a peak in the wavelet transform. The distributions are gaussians because of the intense background flux.

al. , 1993):

$$Y_s(a,b) = \int s(x)\Psi(\frac{x-b}{a})d^2x \tag{1}$$

Since oriented features are not relevant for point sources searches, we will use an isotropic wavelet, the 2D mexican hat. Its bell shape will enhance similar features in the data. It is simply the laplacian of a gaussian:

$$\Psi(x) = (2-|x|^2)\exp(-\frac{1}{2}|x|^2) \tag{2}$$

## 3 Wavelet-transformed data statistics

### 3.1 Density probability function of CWT values

The wavelet transform is also an efficient edge scanner, hence filtering the photon counts map $X$ would yield spurious detections at the discontinuities of the exposure map $\epsilon$. To avoid this, we work with a flat-fielded image, the intensity map $\frac{X}{\epsilon}$. This is relevant for combined maps analysis, but for single viewing periods, we can also work with count maps.

In order to determine the significance of the wavelet transform values of the image, one has to determine the probability density function of the wavelet transform of the background. For a given point $(x,y)$ and a given scale $a$, we have:

$$\hat{f}_{Y_{a,b}} = \exp(\sum_{ij} n_{ij}(e^{ik\frac{\Psi((x_{ij}-b)/a)}{\epsilon_{ij}}} - 1)) \tag{3}$$

where $n_{ij}$ is the expected flux , and $\epsilon_{ij}$ the exposure in pixel (i,j) and $\hat{f}_{Y_{a,b}}$ is the Fourier transform of the probability density function of $Y$ (see appendix for the derivation of this expression).

The probability density function estimation at each point is based on a fast evaluation of formula (3) based on a Taylor expansion of its logarithm. Empirically, this numerical procedure remains accurate as long as the background level is greater than 0.01 photon/bin. If that is not the case, we resort to a full computation of (3). In order to check the validity of these estimates, Monte Carlo simulations have been made and confirm the computations as can be seen in Figure 1.

### 3.2 Thresholds determination

In order to reject wavelet transform values due to the background, one has to set a threshold beyond which a CWT value is considered significant. This threshold is obtained by computing the cumulative probability of $f_{Y_{a,b}}$.

In the above derivation of the probability density function of the background WT, the background and the exposure are nowhere assumed to be uniform, and this is an interesting feature as long as high-energy gamma ray data analysis is concerned. The corrected thresholds values are sometimes substantially different from those found by standard nonparametric methods like Damiani et al. (1997), Starck & Pierre (1998). These latter methods take into account, for the computation of a confidence level at a given point, the correct value of the background at that point, but make the slightly wrong hypothesis of flatness around that point. This can be a disadvantage around a bump in the diffuse emission. Indeed, the thresholds will be underestimated on the peak, and largely overestimated in the negative ring circling the peak. This is illustrated in Figure 2.

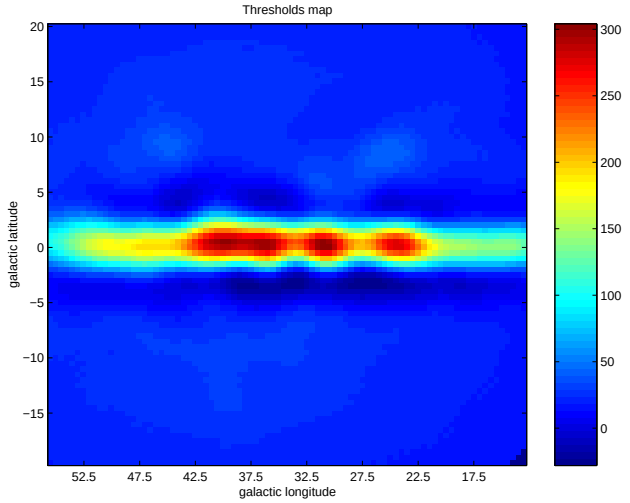


**Fig. 3.** Thresholds map of the EGRET viewing period 20.0 for E>100 MeV and a confidence level of 99.9 %. Note the effect of the strong emission of the galactic plane on the negative values of thresholds around the plane.

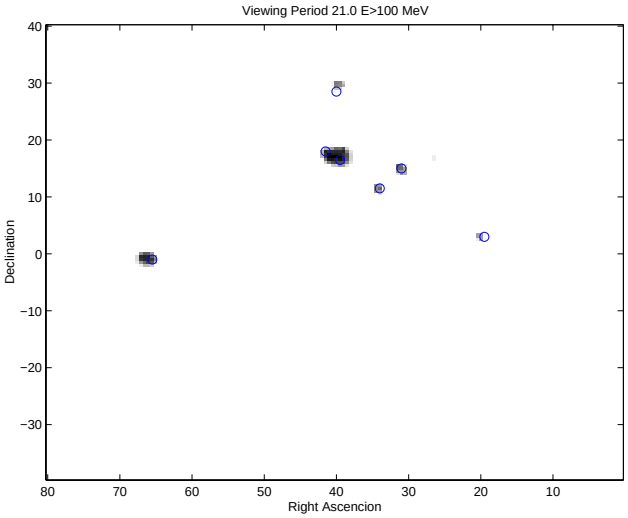


**Fig. 4.** Detected sources using the wavelet analysis of the EGRET viewing period 21.0 for E>100 MeV. Superimposed circles give the positions of the third EGRET catalog sources detected over 3 $\sigma$ (Hartman et al. (1999)). Some small discrepancies on positions remain which are being investigated.

## 4 Source detection

### 4.1 Thresholds maps

Depending on their spectral index, sources won't have the same characteristic scale. Indeed, a source which index is greater than 3 will look much broader in EGRET data than a $E^{-2}$ source. Therefore to detect sources, we need to compute the wavelet transform at several scales in order to search for various PSF sizes. Then for each scale, the wavelet transform values under the given significance threshold are rejected. This gives us a multiscale support see e.g. Starck & Pierre (1998). Then, using the reconstruction by continuous wavelet packets (Torrésani , 1995), we obtain a filtered image yielding the detected sources.

The standard EGRET maps ( 0.5 degrees bins ) were used for this analysis. To compute the threshold map for a given scale $a$, the standard EGRET diffuse background model to which was added the flux of the extragalactic background (Sreekumar et al. , 1998), and the exposure for the considered energy range were used. Figure 3 shows a map obtained for a 99.9 % confidence level for a viewing period centered on the galactic plane.

### 4.2 Application to EGRET viewing period 21.0

Viewing period 21.0 is a high latitude observation in which a bright flaring source (3EG J0237+1635) was detected at 10 $\sigma$ in Hartman et al. (1999) and 16 $\sigma$ in Digel (1999). Several other sources are also present above 3 $\sigma$. The procedure described above has been applied and results are shown on figure 4. We used 0.75, 1, 1.25 and 2 degrees scales to filter and reconstruct the image asking for a 99.9 % confidence level on the wavelet transform values in each pixel. One can see that all the major sources are seen. 3EG J0245+1758, the faint source near 3EG J0237+1635 is not detected, however the bright source indicates a possible source confusion. To see it one would need to add the emission of 3EG J0237+1635 to the model to take into account its effects on the thresholds values.

## 5 Discussion

It has been shown that a wavelet analysis using an isotropic wavelet and a complex and structured background can be used to detect point sources in EGRET data. The algorithm is very efficient for high latitude point-sources, but there are still a few problems to extract all the sources near the galactic plane.

The diffuse emission model used here reproduce the EGRET data very well (Hunter et al. , 1997), therefore using it as the background model is relevant. However, for GLAST, there won't be any model available with sufficient spatial resolution. Many point-like features should be present in the diffuse emission, at a smaller scale than what will be available for the model. One way to handle this problem is to iteratively build the background model from the larger to the smaller scales. This can be done using continuous wavelet packets reconstruction (Torrésani , 1995) for large scales.

Finally, to take into account the spherical geometry of the problem, some studies are undertaken to implement this algorithm for the continuous wavelet transform on the sphere (Antoine & Vandergheynst , 1999).

*Acknowledgements.* R.T. would like to thank Seth Digel for his help and precious advice on EGRET data.

## Appendix A Derivation of the probability density function

The random variable $Y_{a,b}$ of the CWT value at scale $a$ and point $b$ is:

$$Y_{a,b} = \sum_{ij} \frac{N_{ij}}{\epsilon_{ij}} \Psi(\frac{x_{ij} - b}{a}) \quad \text{(A1)}$$

where $N_{ij}$ is the the Poisson random variable of the number of counts in pixel (i,j) of mean value $n_{ij}$. Taking the characteristic function of $Y_{a,b}$, $\hat{f}_{Y_{(a,b)}} = E[e^{ikY_{a,b}}]$, and provided the $N_{i,j}$ are independent, we have:

$$\hat{f}_{Y_{a,b}} = \Pi_{ij} \exp(n_{ij}(e^{ik\frac{\Psi((x_{ij}-b)/a)}{\epsilon_{ij}}} - 1)) \quad \text{(A2)}$$

where $\hat{f}_{Y_{a,b}}$ is the Fourier transform of the probability density function of $Y$. And thus:

$$\hat{f}_{Y_{a,b}} = \exp(\sum_{ij} n_{ij}(e^{ik\frac{\Psi((x_{ij}-b)/a)}{\epsilon_{ij}}} - 1)) \quad \text{(A3)}$$

## References


Antoine, J.P., Carrette, P., Murenzi,R., Piette, B., Image analysis with 2-D continuous wavelet transform, *Signal Processing* **31** (1993) 241-272

Antoine,J.P. , Vandergheynst, P., Wavelets on the 2-sphere : A group-theoretical approach, *Appl. Comput. Harmon. Anal.* **7** (1999) 1-30

Damiani, F., Maggio, A., Micela, G., & Sciortino, S. 1997, Astrophysical Journal, 483, 350

Digel, S. W., Fifth Compton Symposium, Portsmouth, NH, September 1999.

Dixon, D. D., Hartmann, D. H., Kolaczyk, E. D., Samimi, J., Diehl, R., Kanbach, G., Mayer-Hasselwander, H., & Strong, A. W. 1998, New Astronomy, 3, 539

Hartman, R. C. et al. 1999, Astrophysical Journal Supplement, 123, 79

Hunter, S. D. et al. 1997, Astrophysical Journal, 481, 205

Kolaczyk, E. D. & Dixon, D. D. 2000, Astrophysical Journal, 534, 490

Mattox, J. R. et al. 1996, Astrophysical Journal, 461, 396

Sreekumar, P. et al. 1998, Astrophysical Journal, 494, 523

Starck, J. -. L. & Pierre, M. 1998, Astronomy and Astrophysics Supplement, 128, 397

Thompson, D. J. et al. 1993, Astrophysical Journal Supplement, 86, 629

Torrésani, B., *Analyse Continue par Ondelettes*, InterEditions/CNRS Editions, Paris, 1995